



Probabilistic Evaluation of Modeling Parameters for Reinforced Concrete Moment Frame Building

Anil Suwal¹, Hamid Khodadadi Koodiani²(✉), Adolfo Matamoros²,
and Andrés Lepage³

¹ Engineers Design Group, Malden, USA

² The University of Texas at San Antonio, San Antonio, USA
(hamid.khodadadikoodiani, adolfo.matamoros)@utsa.edu

³ The University of Kansas, Kansas, USA
alepage@ku.edu

Abstract. While modeling parameters and acceptance criteria in ASCE 41 are helpful to provide uniformity in the evaluation of different buildings, inconsistencies in their calibration can distort system behavior and location of plastic hinges, and lead to incorrect distributions of damage among building components. Modeling parameters and acceptance criteria for reinforced concrete columns in the ASCE 41–17 standard have undergone significant changes since their inception in early 2000s. The original set of modeling parameters, adopted from FEMA 356 (2000), were updated in a 2007 addendum to incorporate findings from component tests. Modeling parameters and acceptance criteria originally proposed based on engineering judgment were updated to reflect mean values from column tests in ASCE41–17. This study presents fragility relationships for the probability of exceedance of a modeling parameter or component damage state during a seismic hazard event as a function of ground motion intensity. The fragility relationships were developed using nonlinear dynamic analyses of a reinforced concrete building located in Van Nuys, California that was instrumented during several strong earthquakes.

Keywords: Collapse · Earthquake engineering · Fragility relationships · Modeling parameter · Slab-column frames

1 Introduction

Reinforced concrete (RC) buildings built prior to 1970s often have detailing deficiencies because they were designed prior to the development of modern seismic codes. Flexible buildings with components not properly detailed for toughness have a much higher probability of damage and collapse during destructive earthquakes than buildings that comply with the current design provisions for stiffness and detailing. ASCE 41–17 [1] is the current version of a seismic evaluation and rehabilitation standard developed to assist engineers perform seismic assessments of existing buildings based

on a uniform set of criteria. The seismic evaluation process in the standard is based on performance-based engineering concepts, where performance objectives are established through a combination of a desired performance level for a given seismic hazard. This process relies on building numerical models that must have some level of consistency because different assumptions can lead to significantly different outcomes. In the nonlinear dynamic analysis method of the standard, modeling parameters are provided for structural components so moment-rotation and load-deformation relationships in the numerical model are based on uniform criteria. Calculated component demands are compared with acceptance criteria for different performance levels provided in the standard, namely Immediate Occupancy (IO), Life Safety (LS), and Collapse Prevention (CP). In this methodology, building performance is governed by individual elements, and the performance level of the structure is determined by the component with the lowest performance level in the entire structure. Component-based criteria like those in ASCE 41 lack the capability to differentiate building performance on the basis of system-level limit states and do not take into account the capability of structures to redistribute gravity forces after failure of a single component. Two building models, based on modeling parameters in the ASCE 41–13 [2] and ASCE 41–17 [1] standards, were calibrated and evaluated in a companion study and found to provide accurate estimates of roof displacements recorded at the building during the 1994 Northridge Earthquake. These building models were used to perform nonlinear dynamic analyses for the near-fault and far-fault ground motion sets in FEMA P695 [3], normalized to the MCE level earthquake at the building site according to the procedure described in FEMA P695.

The goal of this study is to evaluate modeling parameters and acceptance criteria in the ASCE-41 standard by performing incremental dynamic analyses of numerical models of an existing reinforced concrete building instrumented during several earthquakes, and develop fragility relationships describing the probability of exceedance of modeling parameters and acceptance criteria as a function of earthquake intensity.

Numerical models created in this study represent an existing reinforced concrete building located in Van Nuys, California. The building is unique in that it was instrumented at the time of the 1971 San Fernando earthquake, was heavily instrumented during the 1994 Northridge earthquake, and suffered well-documented heavy column damage during the 1994 Northridge earthquake.

2 Case-Study Building and Its Analytical Model

The case-study building evaluated in this study is a seven-story reinforced concrete frame building located in Van Nuys, CA. The characteristics of the building, the numerical model, detailing of building columns, spandrel beams, and slab-column connections are described in detail by Suwal [4]. Two-dimensional numerical models were created for each of the two principal directions, longitudinal (E-W) and transverse (N-S), using the finite element software OpenSees [5]. Modeling assumptions included rigid floor diaphragms, base columns fixed without including foundation flexibility, building mass lumped at the joints, lumped plasticity with nonlinear rotational springs at each end of structural members, and nonlinear rotational springs with the modified Ibarra-Medina-Krawinkler (IMK) [6] uniaxial material model.

2.1 Modeling Parameters and Acceptance Criteria in Computer Models

Numerical models of the building structure with two different sets of modeling parameters were evaluated in this study. The first had modeling parameters in the ASCE 41–13 standard while the second had modeling parameters in American Concrete Institute (ACI) Committee 369 [7] standard, adopted into ASCE 41–17. The main difference between the two sets of modeling parameters consists of changes in the columns modeling parameters introduced in the ASCE 41–17 standard. Modeling parameters a and b in ASCE 41–13 were calibrated based on test data from rectangular columns with target probabilities of failure of 35% and 15% for flexure-shear and shear critical columns, respectively. Modeling parameters in ACI 369 adopted in ASCE 41–17 included data from circular columns and columns with splices, and had a target probability of failure of 50% for parameters a and b , regardless of the mode of failure.

Modeling parameters provided in tabular form in ASCE 41–13 were replaced by equations in ASCE 41–17, leading to changes in acceptance criteria as well. Instead of plastic rotations corresponding to each performance level, ASCE 41–17 provides acceptance criteria for columns as a fraction of the modeling parameters. Updated values were derived to provide a low probability of exceedance of modeling parameters, while maintaining a similar level of conservatism as the acceptance criteria in ASCE 41–13. Fragility relationships for ASCE 41–13 acceptance criteria were developed using numerical models with ASCE 41–13 modeling parameters and fragility relationships for ASCE 41–17 acceptance criteria were developed with ASCE 41–17 modeling parameters.

2.2 Ground Motion Selection and Scaling

Selection and scaling of ground motions plays a pivotal role in the calculation of fragility relationships. In this study, the procedure in FEMA P695 to determine the collapse margin ratio of buildings was adopted for selection and scaling of ground motions. Both far-fault and near-fault ground motion record sets from FEMA P695, obtained from the PEER NGA database [8], were used in the analyses. The far-fault set comprised records from 22 strong ground motions, while the near-fault set comprised records from 26 ground motions. Only horizontal components were used in this study, so the far-fault set included forty-four different records and the near-fault set included fifty-two different components. As described in FEMA P695, the selection of the ground motions was based on various factors such as magnitude, fault mechanism, site soil conditions, and distance from fault rupture. Two successive scaling procedures were performed for each record. First, ground motion records were normalized by their respective peak ground velocity. After scaling for velocity, records were scaled so the median value of the records matched the MCE hazard level at the fundamental effective period of the building. The fundamental effective period of the case-study building model was found to be 1.71 s in E-W direction and 1.76 s in N-S direction, so the scale factors were slightly different in the E-W and N-S directions, as shown in Figs. 1 and 2. In Figs. 1 and 2 the average response spectrum scaled to the MCE hazard level is shown by the dashed line, and the MCE response spectrum derived from the USGS website is shown by the solid line [9]. The case-study building is located in Van Nuys, CA. The site adjusted MCE level PGA at the building site is 1.028 g. This value was obtained for a class D soil site from the USGS hazard maps [9].

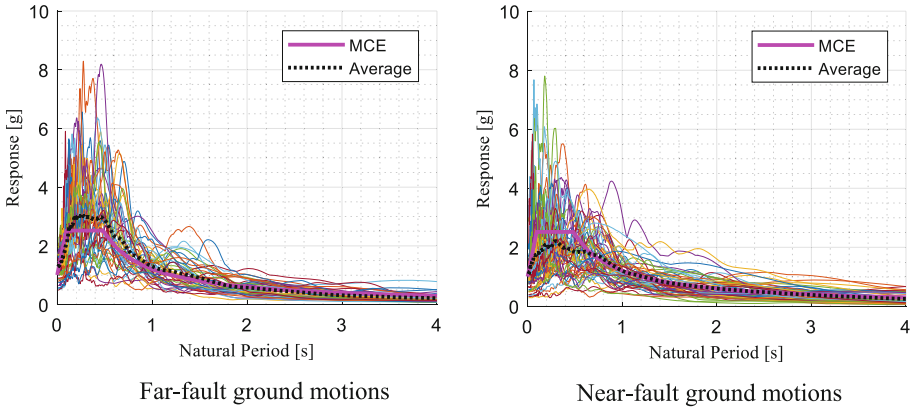


Fig. 1. Scaling of Far-fault and Near-fault ground motions in E-W Direction

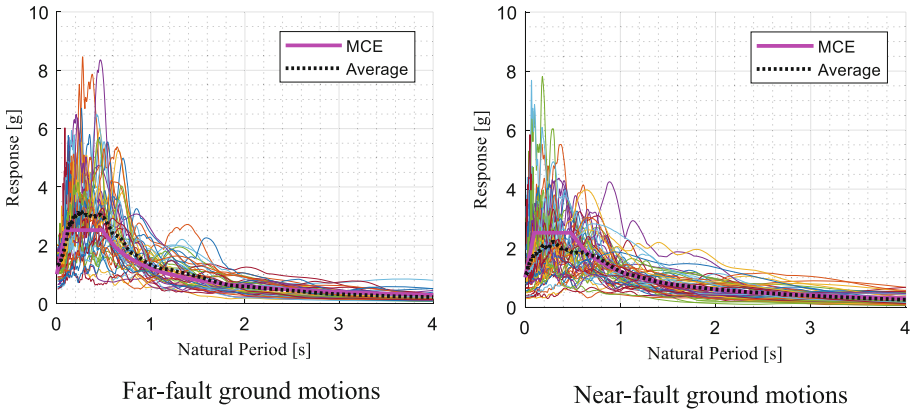


Fig. 2. Scaling of Far-fault and Near-fault ground motions in N-S Direction

2.3 Nonlinear Analyses

Nonlinear dynamic analyses were performed for numerical models with modeling parameters from both ASCE 41–17 and ASCE 41–13, in both the E-W and N-S directions. For each model and each ground motion record, Incremental Dynamic Analyses (IDA) [10] were performed increasing the intensity of shaking until the structure reached collapse due to lateral instability. One of the limitations of the numerical models used in this study is that there was no simulation of loss of gravity load carrying capacity in the columns, so where column rotations exceeded the rotation corresponding to axial failure the material model in the plastic hinge spring maintained axial load carrying capacity while reducing the moment to zero. Another limitation of the modified Ibarra Krawinkler model implementation in OpenSees is that damage in one direction of loading is independent of damage in the other, so columns could exceed the rotation corresponding to axial load failure in one direction while maintaining lateral stiffness in the other. Lateral instability was reached at damage states where column stiffness was severely degraded,

although column rotations could have precipitated local collapse at lower deformations. Deformations indicative of local column collapse are given by fragility relationships for the collapse prevention performance level described later in this study.

IDAs performed in this study were performed with intensity measure increments of 0.05, until the structure was near collapse due to lateral instability, where increments in intensity measure were reduced to 0.01.

3 Probabilistic Assessment of Modeling Parameters

Post-processing of IDA results was performed to extract probabilistic distributions describing the probability of exceedance of modeling parameters, acceptance criteria, and dynamic instability as a function of earthquake intensity. In older reinforced concrete buildings, like the one used for this case study, it is expected that collapse will be controlled by loss of gravity load carrying capacity of a few columns in the building before the building becomes laterally unstable due to the formation of a collapse mechanism. For the case-study building, loss of gravity-load carrying capacity may be precipitated by axial-load failure of columns, punching shear failure of slab-column connections or axial load failure of beam column joints.

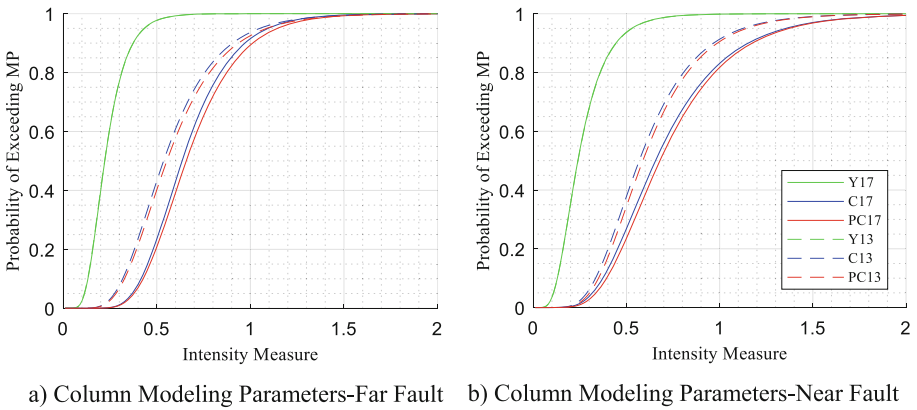
3.1 Fragility Relationships for Modeling Parameters

In non-ductile buildings, local collapse precipitated by elements that sustain severe damage and lose the ability to carry gravity loads is likely to occur at lower intensities of shaking than collapse due to system dynamic instability. For these buildings, the IM at local collapse or at any other element limit state is defined by the number of elements that exceed that limit state within the spatial distribution of inelastic deformations in the structure. In this study, fragility relationships describing the probability of exceedance of element deformation limits were obtained from the results of the incremental dynamic analyses. Calculated rotations for every spring were parsed at all intensity measures to identify the number of springs in the structure below each deformation limit. Fragility curves presented in this study correspond to probabilities of exceedance of at least one spring (plastic hinge) in the structure exceeding a specific limit. Fragility relationships were developed for element subsets to provide insight into the effect that the difference in component criteria has on the performance and assessment of the building system.

3.2 Fragility Relationships for Modeling Parameters in the E-W Direction

Fragility relationships for column modeling parameters of E-W frames are presented in Fig. 3. Dashed lines correspond to fragility relationships for the ASCE 41–13 standard and solid lines correspond to the ASCE 41–17 standard. Figure 3 (a) and 3(b) present fragility relationships corresponding to far-fault and near-fault ground motion sets, respectively. In both Fig. 3 (a) and Fig. 3 (b), fragility relationships corresponding to the yield point (green lines in the figures) according to the ASCE 41–17 and ASCE 41–13 standards were exactly the same for both the far-fault and near-fault ground motion sets which is to be expected because the difference between the two standards is in modeling

parameters *a* (inelastic rotation at the capping point) and *b* (inelastic rotation at loss of gravity load capacity), while effective stiffness values are the same in both standards. Fragility relationships corresponding to capping and post-capping modeling parameters (*a* and *b*) for the ASCE 41–17 model were slightly to the right of the curves for the ASCE 41–13 model, for both ground motion sets. An increase of almost 10% on the intensity measure corresponding to the mean probability of exceedance was observed for the ASCE 41–17 model with respect to the ASCE 41–13 model, for capping and post-capping modeling parameters, for both sets of ground motions. For example, for the far-fault ground motion set, the intensity measure at the mean probability of exceeding the capping modeling parameter was 0.53 for the ASCE 41–13 model, while it was 0.62 for the ASCE 41–17 model (increase of 0.1). Similarly, the intensity measure at the mean probability of exceedance for the post-capping modeling parameter was 0.54 for the ASCE 41–13 model and 0.67 for the ASCE 41–17 model. The capping and post-capping fragility curves for both models (dashed and solid line in the Fig. 3) were very close to each other, which indicates that the post-capping limit point, indicative of loss of gravity load carrying capacity, was reached at small increments of IM with respect to the capping limit point. Furthermore, near fault fragility curves were flatter than far fault fragility curves, with the difference between the two becoming noticeable at probabilities of exceedance greater than 50%. For a probability of exceedance of 80%, the IM corresponding to axial failure (post capping point) was approximately 0.88 for the far-fault set and 0.98 for the near-fault set, with a greater difference between the ASCE 41–17 and ASCE 41–13 models for the far-fault set than the near-fault set.



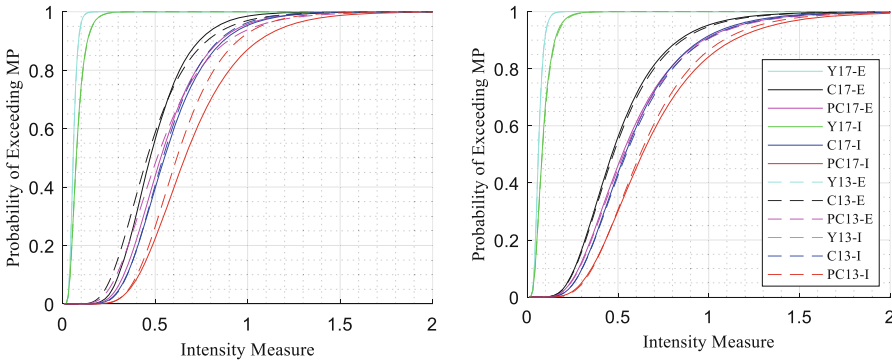
Note: Y17, C17 and PC17 refers to yield, capping and post-capping modeling parameters of ASCE 41-17

Y13, C13 and PC13 refers to yield, capping and post-capping modeling parameters of ASCE 41-13

Fig. 3. Probability of exceedance of column Modeling Parameters for Far-Fault and Near-Fault ground motion sets, E-W frame models

A very important finding from this study is that Calculated fragility curves for beams were to the left of fragility curves for columns, meaning that the probability of exceeding all modeling parameters was higher for beams than it was for columns. Another important observation is that while fragility relationships for capping and post-capping modeling parameters of columns were nearly the same for both standards (Fig. 3), there was an observable difference between the fragility curves for capping and post-capping modeling parameters of beams, which increased with IM.

One of the reasons this building was selected for the study was that its moment frames have three different types of elements: columns, beams, and flat slabs. Having different types of moment frame elements permits evaluating the effect of using different element calibration criteria on the evaluation outcome for the system. With that objective in mind, the beam subset was divided into subsets of spandrel beams located in the exterior frames and slabs in the interior frames. Figure 4 (a) shows fragility relationships for modeling parameters of exterior and interior frame beams. Although fragility curves for the yield point were the same for both standards, exterior frame beams had higher probabilities of exceedance than interior frame beams (Fig. 4). Similarly, capping and post-capping rotations had a higher probability of exceedance for exterior than for interior frames (Fig. 4 (a) and 4(b)). Figure 4 (b) shows fragility relationships corresponding to the three modeling parameters for interior and exterior beams subjected to the near-fault ground motion set. The main difference between Fig. 4 (a) and 4(b) is that the gap between the fragility relationships corresponding to the post-capping modeling parameter for ASCE 41–13 and ASCE 41–17 models was negligible for the near-fault ground motion set while it was not negligible for the far-fault ground motion set. For all other cases the gap between fragility curves for the ASCE 41–13 and ASCE 41–17 models were very small. It should be noted that.



a) Interior & Exterior Beam MP, far-fault b) Interior & Exterior Beam MP, near-fault

Note: Y, C and PC refers to yield, capping and post-capping
 E and I refers to exterior beam and interior beam
 17 and 13 refers to modeling parameters of ASCE 41-17 and ASCE 41-13.

Fig. 4. Probability of exceedance for interior and exterior frame beam modeling parameters as a function of IM for far-fault and near-fault ground motion sets, E-W direction

3.3 Fragility Relationships for N-S Frame Modeling Parameters

Fragility relationships corresponding to ASCE 41–17 and ASCE 41–13 modeling parameters of columns were developed for N-S frames also (Fig. 5). Simulations for ASCE 41–13 model were only performed for the far-fault ground motion sets due to the large computational cost and storage required for an IDA of a ground motion set. Fragility relationships corresponding to all modeling parameters differed significantly between the ASCE 41–17 model and the ASCE 41–13 model, as shown in Fig. 5 (b) (dashed and solid blue line). Figure 5 (b) shows that, for ASCE 41–17 model, the gap between fragility curves corresponding to yield and capping modeling parameters was greater than the gap between fragility curves corresponding to capping and post-capping modeling parameters. The opposite was true for the ASCE 41–13 model, where the gap between fragility curves corresponding to capping and post capping was far greater than the gap between fragility curves corresponding to yield and capping modeling parameters. Probabilities of exceedance for the N-S frame models were significantly higher than probabilities of exceedance for E-W frames. Intensity measures for the mean probability of exceedance of E-W frames were approximately 0.68 for the post-capping point and capping point of the ASCE 41–17 model and 0.58 for the capping point and post capping point of the ASCE 41–13 model.

Fragility relationships for the exterior and interior beams of N-S frames for both models are shown in the Fig. 6. Similar to frames in the E-W direction, probabilities of exceedance of modeling parameters for exterior frame beams were higher than probabilities of exceedance for interior frame beams.

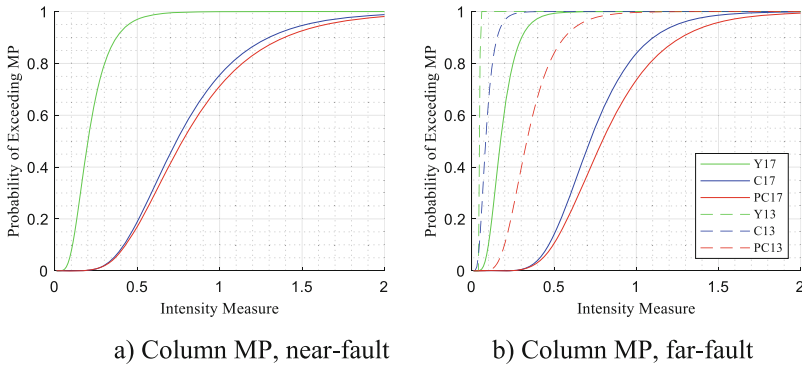
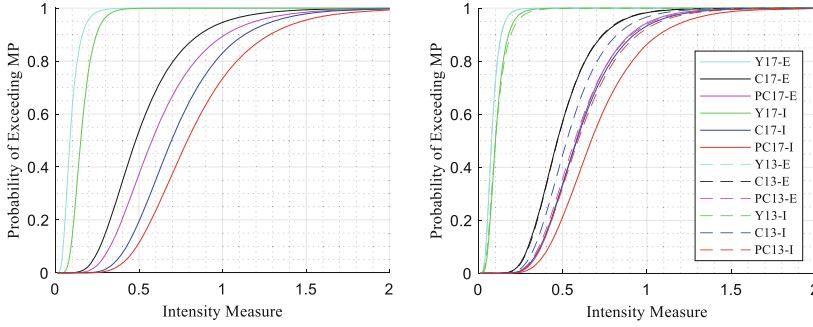


Fig. 5. Probability of exceedance of column modeling parameters for N-S frames subjected to near-fault and far-fault ground motion sets



a) Exterior & interior beam MP, near fault b) Exterior & interior beam MP, far-fault

Fig. 6. Probability of exceedance for beam modeling parameters as a function of intensity measure, N-S frames subjected to near-fault and far-fault ground motions

4 Conclusions

Seismic fragility relationships corresponding to column modeling parameters changed as a result of changes in modeling parameters introduced into the ASCE 41–17 standard. Because changes in the standard did not affect the yield point, fragility relationships corresponding to column yield point were the same for the ASCE 41–17 and ASCE 41–13 standard models, for both the far-fault and near-fault ground motion sets. Fragility relationships for column capping and post-capping modeling parameters obtained with the ASCE 41–17 standard shifted towards right of those obtained with the ASCE 41–13 standard, which means that the probability of exceedance for the capping and post-capping column modeling parameters had a lower exceedance probability for the ASCE 41–17 standard than the ASCE 41–13 standard. A similar change was observed for the near-fault and far-fault ground motion sets, although models corresponding to both standards had higher probabilities of exceedance for the far-fault ground motion set than the near-fault ground motion set.

Fragility relationships corresponding to the interior and exterior frame beam modeling parameters showed that interior frame beams (slab-column connections) had lower probabilities of exceedance than exterior frame beams. Exterior frame beams had the highest probability of exceedance of all elements, both for the near-fault and far-fault ground motion sets. The fragility relationship corresponding to beam modeling parameters showed that the probability of exceedance of all beam modeling parameters was nearly the same for the near-fault and far-fault ground motion sets.

For the far-fault ground motion set, columns had a higher intensity measure at the mean probability of exceedance for the yield, capping, and post-capping points than beams. Calculated fragility curves for beams were to the left of fragility curves for columns, meaning that the probability of exceeding all modeling parameters was higher for beams than it was for columns. This trend is consistent with the reduction in the level of conservatism of column capping and post-capping modeling parameters in the ASCE 41–17 standard, while beam and slab-column connection modeling parameters remained the unchanged. For capping and post-capping, fragility relationships for beam

modeling parameters were nearly the same for ASCE 41–13 and ASCE 41–17 models, which indicates that the change in the column modeling parameters did not affect the probability of exceedance of beam modeling parameters. For both models, the probabilities of exceedance for beams modeling parameters were higher than probabilities of exceedance for column modeling parameters for capping and post-capping, which indicates higher inelastic deformation demands in beams than in the columns.

References

1. American society of civil engineers/structural engineering institute (ASCE/SEI) (2017) Committee 41, seismic evaluation and retrofit of existing buildings
2. American society of civil engineers/structural engineering institute (ASCE/SEI) (2013) Committee 41, seismic evaluation and retrofit of existing buildings
3. Federal emergency management agency, FEMA P-695 (2009) Quantification of seismic performance factors. Washington, DC
4. Suwal, A (2018) Performance evaluation of a non-ductile reinforced concrete moment frame building. Doctoral dissertation, The University of Texas at San Antonio, San Antonio, Texas
5. OpenSees (2006) Open system for earthquake engineering simulation
6. Ibarra LF, Medina RA, Krawinkler H (2005) Hysteretic models that incorporate strength and stiffness deterioration. *Earthq Eng Struct Dynam* 34(12):1489–1511
7. American Concrete Institute (ACI) Committee 369.1 (2017). Standard requirements for seismic evaluation and retrofit of existing concrete buildings
8. The pacific earthquake engineering research center (PEER, N.D.) (2014). University of California at Berkeley. <https://peer.berkeley.edu/peer-strong-ground-motion-databases>
9. United States Geological Survey. <https://www.usgs.gov>
10. Vamvatsikos D, Cornell CA (2002) Incremental dynamic analysis. *Earthq Eng Struct Dynam* 31(3):491–514